https://doi.org/10.37434/tpwj2022.03.01

CHARACTERISTICS OF HIGH-FREQUENCY PULSED CURRENT ARC WITH REFRACTORY CATHODE

I. Krivtsun[1], V. Demchenko[1], I. Krikent[1], U. Reisgen[2], O. Mokrov[2], R. Sharma[2]

[1]E.O. Paton Electric Welding Institute of the NASU
11 Kazymyr Malevych Str., 03150, Kyiv, Ukraine
[2]RWTH Aachen University, ISF – Welding and Joining Institute
Pontstr. 49, 52062, Aachen, Germany

ABSTRACT

A self-consisted mathematical model is presented, describing nonstationary processes of energy, momentum, mass and charge transfer in plasma column and anode boundary layer of an electric arc burning in atmospheric pressure inert gas at pulsed modulation of current. A numerical study of distributed and integrated characteristics of 2 mm long argon arc was performed in the case of current modulation by rectangular pulses at 10 kHz frequency and different values of the duty cycle (0.3; 0.5; 0.7) under the condition that the average current value remains unchanged and equal to 140 A. Calculated time dependencies of plasma temperature, velocity and current density in the arc column centre, as well as axial values of plasma temperature and pressure near the anode surface, anode current density and heat flux into the anode are given for the selected values of duty cycle. Radial distributions of averaged over the current modulation period heat flux, introduced by the arc into the anode, pressure and force of friction of arc plasma flow on its surface were calculated, which are the determinant ones for simulation of thermal and hydrodynamic processes in the metal being welded in TIG welding with high-frequency pulsed current (HFPC) modulation. Results of simulation of nonstationary arc characteristics are compared with the respective results for a direct current (DC) arc, at current equal to average value of modulated current. Analysis of the obtained results leads to the conclusion that in the case of HFPC TIG welding at 10 kHz frequency decrease of duty cycle (increase of pulse current) at constant value of average current leads to greater force impact of such an arc on weld pool metal and to increase of its penetrability, respectively.

KEYWORDS: electric arc, refractory cathode, arc column, anode boundary layer, TIG welding, pulsed current modulation, frequency, duty cycle, simulation

INTRODUCTION

TIG welding currently is one of the main technological processes of producing high-quality permanent joints of critical structures from steels, titanium and aluminium alloys. This welding process is realized by excitation of DC electric arc in inert shielding gas (Ar, He or their mixture) between refractory (W) cathode and item being welded, which is the anode [1].

There are different modifications of TIG welding, one of which is welding current modulation. A large number of works are devoted to experimental study of the features of this process (see, for instance, [2–8]). Modes of TIG welding with low-frequency (modulation frequency $f \leq 50$ Hz) [2, 3, 4, 7, 8]), medium-frequency ($f \sim 5$ kHz) [3, 4]) and high-frequency ($f \geq 10$ kHz) [3, 5, 6]) arc current modulation were investigated. Results of these studies lead to the conclusion that variation of such parameters of welding current modulation as frequency, pulse ratio, amplitude and shape of the pulses, allows controlling the metal penetration shape, and thermal cycle of welding and, therefore, influencing the structure and properties of metal of the weld and heat-affected zone.

Works [9–11] are devoted to theoretical study and computer simulation of the processes, running in the welding arc and metal being welded in TIG welding with low-frequency pulsed current modulation. The problems of simulation of distributed and integrated characteristics of arc plasma and its impact on the metal being welded in HFPC TIG welding are not given enough attention in modern scientific and technical publications. Therefore, the objective of this work is numerical analysis of nonstationary processes of energy, momentum, mass and charge transfer in the arc with a refractory cathode at HFPC modulation in the range of 30–400 A by rectangular pulses at 10 kHz frequency.

Let us consider a nonstationary electric arc with a refractory cathode and water-cooled (nonevaporating) anode, burning in atmospheric pressure inert gas, the diagram of which is shown in Figure 1. At construction of a mathematical model of such an arc, we will give the main attention to processes running in the column and anode boundary layer of arc plasma. For self-consistent description of the above-mentioned processes, we will use an approach, described in detail in [12], according to which we will divide arc plasma into two regions: arc column, where plasma is in the state of local thermodynamic equilibrium and anode boundary layer of thermally and ionizationally nonequilibrium plasma. Accordingly, a self-consistent mathematical model of the considered system should include two interrelated models:

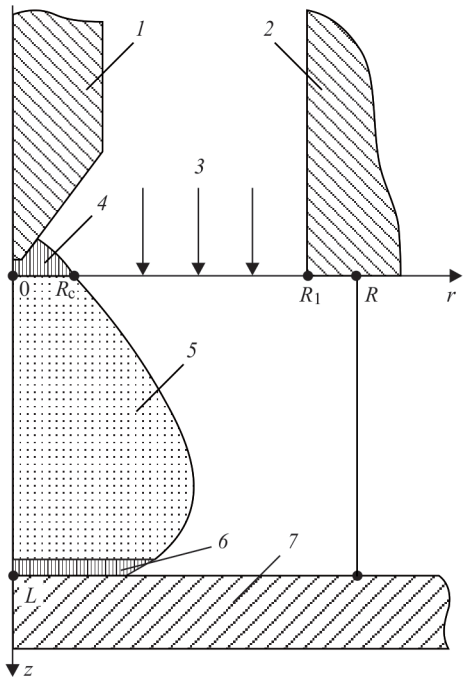

Figure 1. Diagram for simulation of a nonstationary arc: *1* — refractory cathode; *2* — nozzle for shielding gas feeding; *3* — shielding inert gas; *4* — cathode region; *5* — arc column; *6* — anode boundary layer; *7* — water-cooled anode; R_c — radius of the region of the arc cathode attachment; R_1 — protective nozzle radius; R — calculation domain radius, L — arc length

● Model of nonstationary thermal, electromagnetic and gas-dynamic processes in arc column plasma at pulsed current modulation.

● Model of anode boundary layer, allowing formulation of boundary conditions on the interface of plasma column with the above layer, which, on the one hand, are required to solve the equations of the first model, and on the other hand they are needed for determination of the characteristics of thermal, electric and force impact of a nonstationary arc on the anode surface.

MODEL OF NONSTATIONARY ARC COLUMN

At construction of the model of thermal, electromagnetic and gas-dynamic processes in arc column plasma at pulsed modulation of current, we will use the following approximations:

● the system is assumed to be axisymmetric, anode surface is flat and is perpendicular to the arc axis;

● arc column plasma contains only shielding gas particles (electrode material evaporation is neglected), it is in the state of local thermodynamic equilibrium (one-temperature model of ionizationally equilibrium plasma is used) and it is optically thin for intrinsic radiation;

● main mechanism of plasma heating is Joule heating (work of pressure forces and viscous dissipation are ignored), while energy transfer in arc column takes place through thermal conductivity, convection and transport of energy of the plasma electron component;

● electromagnetic processes in arc plasma are assumed to be quasistationary (bias currents are neglected);

● arc column plasma flow is viscous, subsonic, flow mode is laminar;

● gravitational force is neglected, external magnetic fields are absent.

The corresponding to these approximations system of differential equations for description of nonstationary processes in arc column plasma, written in the cylindrical system of coordinates {r, φ, z} has the following form:

● Mass conservation equation

$$\frac{\partial \rho}{\partial t}+\frac{1}{r}\frac{\partial}{\partial r}(r\rho v)+\frac{\partial}{\partial z}(\rho u)=0, \qquad (1)$$

where ρ is the mass density of plasma; v, u are the radial and axial components of its velocity.

Equations of momentum conservation

$$\rho\left(\frac{\partial v}{\partial t}+v\frac{\partial v}{\partial r}+u\frac{\partial v}{\partial z}\right)=-\frac{\partial P}{\partial r}-$$

$$-j_z B_\varphi+\frac{2}{r}\frac{\partial}{\partial r}\left(r\eta\frac{\partial v}{\partial r}\right)+\frac{\partial}{\partial z}\left[\eta\left(\frac{\partial u}{\partial r}+\frac{\partial v}{\partial z}\right)\right]- \qquad (2)$$

$$-2\eta\frac{v}{r^2}-\frac{2}{3}\frac{\partial}{\partial r}\left\{\eta\left[\frac{1}{r}\frac{\partial\left(rv\right)}{\partial r}+\frac{\partial u}{\partial z}\right]\right\};$$

$$\rho\left(\frac{\partial u}{\partial t}+v\frac{\partial u}{\partial r}+u\frac{\partial u}{\partial z}\right)=-\frac{\partial P}{\partial z}+$$

$$+j\ B\ +\ \frac{\partial}{\partial z}\left(\eta\frac{\partial u}{\partial z}\right)+\frac{1}{r}\frac{\partial}{\partial r}\left[r\eta\left(\frac{\partial u}{\partial r}+\frac{\partial v}{\partial z}\right)\right]- \qquad (3)$$

$$-\frac{2}{\partial z}\left\{\eta\left[\frac{1}{r}\frac{\partial\left(rv\right)}{\partial r}+\frac{\partial}{\partial z}\right]\right\}$$

where P is the pressure; j_z, j_r are the axial and radial components of current density in the arc; B_φ is the azimuth component of magnetic induction vector; η is the coefficient of dynamic viscosity. Since the pressure can be determined up to the constant, let's choose such a constant from the condition that pressure in external media corresponds to atmospheric one. The

value P should be understood below to refer to overpressure.

● Energy conservation equation

$$\rho C_p\left(\frac{\partial T}{\partial t}+v\frac{\partial T}{\partial r}+u\frac{\partial T}{\partial z}\right)= =\frac{1}{r}\frac{\partial}{\partial r}\left(r\chi\frac{\partial T}{\partial r}\right)+\frac{\partial}{\partial z}\left(\chi\frac{\partial T}{\partial z}\right)+\frac{k}{e}\times \times\left\{j_r\frac{\partial\left[(5/2-\delta)T\right]}{\partial r}+j_z\frac{\partial\left[(5/2-\delta)T\right]}{\partial z}\right\}+ +\frac{j_r^2+j_z^2}{\sigma}-\psi, \quad (4)$$

where C_p is the specific heat of arc plasma, allowing for ionization energy; T is the plasma temperature; χ is the coefficient of thermal conductivity; k is the Boltzmann constant; e is the electron charge; δ is the thermal diffusion constant; ψ are the radiation energy losses.

● Equations of electromagnetic field

$$\frac{1}{r}\frac{\partial}{\partial r}\left(r\sigma\frac{\partial\varphi}{\partial r}\right)+\frac{\partial}{\partial z}\left(\sigma\frac{\partial\varphi}{\partial z}\right)=0; \quad (5)$$

$$B_\varphi(r,z)=\frac{\mu^0}{r}\int_0^r j_z(\xi,z)\,\xi\,d\xi, \quad (6)$$

where φ is the electric potential; σ is the specific heat conductivity of plasma; μ^0 is the universal magnetic constant;

$$j_r=-\sigma\frac{\partial\varphi}{\partial r}; \qquad j_z=-\sigma\frac{\partial\varphi}{\partial z}. \quad (7)$$

Before we go over to consideration of the initial and boundary conditions for equations (1)–(5), we will briefly describe the model of the arc anode boundary layer used in this paper.

MODEL OF ANODE BOUNDARY LAYER

According to the model proposed in [12, 13], the anode boundary layer is assumed to be infinitely thin, compared to arc column dimensions, and potential drop in this layer (anode drop) $U_a = \varphi_a - \varphi_{pa}$ is negative and its distribution along the anode surface is nonuniform. Here, φ_a is the anode surface potential assumed to be constant, in view of the high conductivity of the anode metal, and selected equal to zero further on, while φ_{pa} is the potential of arc column plasma on the interface with the anode boundary layer, the value of which depends on distance r to the arc axis for an axisymmetric arc. To calculate the radial distribution of plasma potential on the above-mentioned interface, we will use expression [13], which in the case of nonevaporating anode (arc plasma contains just the atoms and single-charged ions of shielding gas) can be written in the following form

$$\varphi_{pa}(r)=\frac{kT(r,L)}{e}\ln\left(\frac{e n_e(r,L)\bar{\upsilon}_e(r,L)}{4\left[j_a(r)+j_i(r)\right]}\right), \quad (8)$$

where $T(r, L)$, $n_e(r, L)$, $\bar{\upsilon}_e(r,L)=\sqrt{8kT(r,L)/\pi m_e}$ are the radial distributions of temperature, concentration and thermal velocity of plasma electrons on the interface of the arc column with the anode boundary layer, m_e is the electron mass; $j_a(r) = |j_z(r, L)|$, $j_i(r)=en_i(r,L)\exp\left(-\frac{1}{2}\right)\sqrt{\frac{k\left[T(r,L)+T_s\right]}{M}}$ are the respective distributions of normal to the anode surface component of the density of the arc anode current and ion current from the plasma to anode surface, $n_i(r, L)$ is the distribution of plasma ion concentration on the interface of the arc column with the anode boundary layer, M is the ion mass, T_s is the anode surface temperature. Taking into account the above assumption of ionisational equilibrium of arc column plasma, the distributions of $n_e(r, L)$, $n_i(r, L)$ and the respective atom concentration $n_a(r, L)$ can be calculated, using Saha equation, plasma quasineutrality condition and law of partial pressures [13].

We will present the heat flux from the plasma to the anode surface as follows: $q_{pa} = q_e + q_i$, where q_e, q_i are the flows of kinetic and potential energy, transferred by electrons and ions of plasma, respectively. To calculate the radial distributions of the above quantities, we will use expressions [12], which in the case of a nonevaporating anode can be written in the following form:

$$q_e(r)=j_e(r)\frac{5kT(r,L)}{2e}; \quad (9)$$

$$q_i(r)=j_i(r)\left[\varphi_{pa}(r)+\frac{1}{2}\frac{kT_s}{e}+U_i\right]. \quad (10)$$

Here,

$$j_e(r)=\frac{1}{4}en_e(r,L)\bar{\upsilon}_e(r,L)\exp\left[-\frac{e\varphi_{pa}(r)}{kT(r,L)}\right]$$

is the electron current from the plasma to the anode surface; U_i is the ionisation potential of shielding gas atoms. It should be noted that the distribution of the full heat flux into the anode should be calculated, allowing for electron work function ζ_a that yields:

$$q_a(r) = q_{pa}(r) + j_a(r)\zeta_a. \qquad (11)$$

Thus, the proposed model of the arc anode boundary layer allows calculation of the distributions of the anode potential drop $U_a(r)$ and density $q_a(r)$ of the heat flux introduced into the anode, depending on the kind of shielding gas, distributions of anode current density and arc column plasma temperature on the interface with the anode boundary layer, as well as anode surface temperature T_s. In its turn, the distributions of $j_a(r)$ and $T(r, L)$ quantities can be determined, proceeding from the arc column model with self-consistent boundary conditions on the anode.

In completion of the description of anode boundary layer model, we will note that its application in the case of a nonstationary arc requires allowing for the dependencies of all the quantities, included into relationships (8)–(11), not only on radial coordinate *r*, but also on time *t*. Estimating the relaxation time of the anode boundary layer characteristics using relationship $\tau_a \sim /l_a/\bar{\upsilon}_e$, where l_a is the layer thickness, $\bar{\upsilon}_e$ is the thermal velocity of electrons, the values of which for atmospheric pressure argon arc are equal to $5\cdot10^{-4}$ m and $5\cdot10^5$ m/s, respectively [14], we obtain $\tau_a \sim 10^{-9}$ s, that is much smaller than the time for the change of arc column plasma characteristics $\tau_p \sim 10^{-4}$ s [15] and the period of current change at the considered modulation frequency. Thus, the above-given relationships are quite applicable to the description of anode processes running in the considered arc, allowing for the fact that the included into them distributed characteristics of arc plasma on the interface with the anode boundary layer appropriately depend on time.

INITIAL AND BOUNDARY CONDITIONS FOR A NONSTATIONARY ARC MODEL

Appropriate initial and boundary conditions should be assigned to solve the system of differential equations (1)–(5), describing nonstationary processes of heat-, mass- and charge transfer in the arc column. As the fields of arc plasma temperature and velocity are set fast enough (as shown by calculations [16], 6–8 pulses are sufficient in order to achieve a periodical change of characteristics of the above-mentioned fields at about 10 kHz frequency of arc current pulsed modulation), initial distributions of plasma velocity and temperature are of no fundamental importance. For instance, zero values can be set for velocity components, and plasma temperature in the current channel area should be selected so as to ensure the plasma conductivity characteristic for an argon arc.

In the case considered here of a nonstationary arc with the tungsten cathode and water-cooled (nonevaporating) anode, we will formulate boundary conditions for sought functions (v, u, P, T, φ) as follows.

Near the cathode (plane $z = 0$ in Figure 1) the conditions for the components of the velocity vector are set as follows:

$$v|_{z=0} = 0; \quad u|_{z=0} = \begin{cases} u\ , 0 \le r < R\ ; \\ 0, R\ \le r \le R, \end{cases} \qquad (12)$$

where quantity u_0 is determined by shielding gas flow rate and radius R_1 of its feeding nozzle (see Figure 1).

For temperature and electric potential in the zone of cathode attachment of a nonstationary arc (at $0 \le r \le R_c$, $z = 0$) we will take the following conditions

$$T|_{z=0} = T_c(r,t); \quad \sigma \left.\frac{\partial \varphi}{\partial z}\right|_{z=0} = j_c(r,t), \qquad (13)$$

where $T_c(r, t)$, $j_c(r, t)$ are the radial distributions of plasma temperature and current density near the cathode, changing in time at arc current modulation, the explicit form of which, following [17], is set as follows:

$$j_c(r,t) = j_{c0}(t)\frac{1}{2}erfc\left\{\frac{10\left[r - r_{0c}(t)\right]}{r_{0c}(t)}\right\} \qquad (14)$$

and similarly for $T_c(r, t)$, taking into account the fact that shielding gas temperature is equal to ambient temperature T_0 outside the region of cathode attachment of the arc ($r > R_c$). Here, $j_{c0}(t)$ is the axial value of current density; $erfc(x) = \frac{2}{\sqrt{\pi}} \int_x^\infty e^{-y^2} dy$; $r_{0c}(t)$ is the distance from the arc axis, where current density drops two times.

Estimating the time for setting of cathode layer characteristics τ_c using relationship $\tau_c \sim L_c/\bar{\upsilon}_e$ where L_c is the layer thickness, $\bar{\upsilon}_e$ is the mean thermal velocity of electrons in this layer, the values of which we will select equal to $3\cdot10^{-4}$ m and $1.2\cdot10^6$ m/s in the case of atmospheric pressure argon arc with a tungsten cathode [18], we will obtain $\tau_c \sim 2.5\cdot10^{-10}$ s. As this time is much shorter than the period of arc current variation at modulation frequency $f = 10$ kHz, we will assume that radial distributions of current density and plasma temperature near the cathode completely follow the change of arc current at considered f value. Thus, we will assign the axial values of current density $j_{c0}(t)$ and near-cathode plasma temperature $T_{c0}(t)$ at each moment of time according to recommendations of work [17], depending on the instantaneous value of arc current, determined by the law of its modulation $I(t)$. Selecting radius $R_c(t)$ of the zone of cathode attachment of the arc (see Figure 1) as the distance from its axis, at which current density is less than 1 %

of j_{c0} at the respective moment of time, and allowing for (14), we have $R_c(t) = 1.165 r_{0c}(t)$. Here, the time dependence of quantity r_{0c} can be found from the integral relationship for total current.

$$I(t) = 2\pi \int_0^\infty r j_c(r,t) dr. \quad (15)$$

Outside the zone of cathode attachment of the arc (at $R_c < r \le R$, $z = 0$) we assume:

$$T|_{z=0} = T_0; \quad \left.\frac{\partial \varphi}{\partial z}\right|_{z=0} = 0. \quad (16)$$

On the anode surface (plane $z = L$ in Figure 1) we accept the "sticking" conditions

$$v|_{z=L} = u|_{z=L} = 0. \quad (17)$$

On the interface of arc column plasma with the anode boundary layer, or considering the assumption made of its infinitely small thickness, at $z = L$, the following condition of energy balance can be used as the boundary condition:

$$\left[-\chi \frac{\partial T}{\partial z} + |j_z| \frac{k}{e}\left(\frac{5}{2} - \delta\right) T\right]_{z=L} = \varphi_{pa}(r,t) j_a(r,t) + q_{pa}(r,t). \quad (18)$$

As the electric potential of the anode surface is assumed to be constant and equal to zero, the boundary condition for plasma potential on the interface of the arc column with the anode boundary layer can be written as follows:

$$\varphi|_{z=L} = \varphi_{pa}(r,t). \quad (19)$$

Boundary conditions for plasma velocity, temperature and electric potential on the axis of system symmetry are set in a standard way

$$v|_{r=0} = 0; \quad \left.\frac{\partial u}{\partial r}\right|_{r=0} = \left.\frac{\partial T}{\partial r}\right|_{r=0} = \left.\frac{\partial \varphi}{\partial r}\right|_{r=0} = 0. \quad (20)$$

On the outer boundary of the calculated region ($r = R$) for plasma velocity and electric potential we can write

$$\left.\frac{\partial(\rho v r)}{\partial r}\right|_{r=R} = 0; \quad u|_{r=R} = 0; \quad \left.\frac{\partial \varphi}{\partial r}\right|_{r=R} = 0. \quad (21)$$

We will determine the boundary condition for plasma temperature at $r = R$, depending on the flow direction

$$T|_{r=R} = T_0, \text{ at } v|_{r=R} \le 0; \quad \left.\frac{\partial T}{\partial r}\right|_{r=R} = 0, \text{ at } v|_{r=R} > 0. \quad (22)$$

The system of differential equations (1)–(5) with above-described initial and boundary conditions was solved numerically, by the method of finite differences, using the joint Euler–Lagrange method, adapted to the conditions of the compressible medium. Calculated data from works [19, 20] were used to determine the temperature dependencies of thermodynamic characteristics, transport coefficients and losses of energy for arc plasma radiation, included into the model equations.

SIMULATION RESULTS

As the object of numerical study, we will select a nonstationary arc with a refractory cathode, burning under the conditions characteristic for HFPC TIG welding. We will assume that arc current $I(t)$ is unipolar ($I(t) \ge 0$), and its modulation is performed by rectangular pulses in the range of $I_1 < I(t) < I_2$, where I_1 is the pause current; I_2 is the pulse current (modulation amplitude $A = I_2 - I_1$), with pulses following with frequency f (modulation period $T_m = 1/f$) at different values of duty cycle δ, characterizing the ratio of pulse duration to modulation period. Average I_{av} and effective I_{eff} values of arc current can be determined as follows:

$$I_{av} = \langle I(t) \rangle; \quad I_{eff} = \sqrt{\langle I^2(t) \rangle},$$

where

$$\langle \phi(t) \rangle = \frac{1}{T_m} \int_0^{T_m} \phi(t) dt$$

is the integral mean value of periodic function $\phi(t)$ in interval $t \in [0; T_m]$.

We will consider a nonstationary arc of length $L = 2$ mm with a refractory cathode and water-cooled (nonevaporating) anode, burning in atmospheric pressure argon, at the following parameters of HFPC modulation: frequency $f = 10$ kHz ($T_m = 100$ μs); duty cycle $\delta = 0.3$; 0.5 (meander); 0.7; pause current $I_1 = 30$ A, and we will determine the respective value of pulse current I_2 from the condition that average value of arc current I_{av} remains constant and equal to 140 A at all values of δ. The obtained values of I_2, A, I_{eff} are given in Table 1.

Results of calculation of the distributed and integrated characteristics of the considered arc and its impact of the anode surface at the given parameters of current modulation were compared with the calculated values of the respective characteristics of a DC arc, at current equal to average value of modulated current.

Figure 2 shows the change in time of arc plasma temperature T_0, its velocity u_0 and current density $j_0 = |j_{0z}|$ on the arc column axis ($r = 0$) in section $z = 1$ mm (midpoint of arc length). In these figures and further on the solid curves marked by numbers 1, 2, 3, correspond to duty cycles $\delta = 0.3$; 0,5; 0.7; dashed

Table 1. Parameters of arc current modulation

δ	I_2, A	A, A	I_{eff}, A
0.3	396.7	366.7	218.7
0.5	250.0	220.0	178.0
0.7	187.1	157.1	157.4

lines are the respective values for DC arc (I = 140 A); time is counted from the beginning of the pause.

Calculations show that under the considered conditions, values T_0, u_0 and j_0 turn out to be significantly greater during the current pulse, than during the pause, and the more so, the smaller is the duty cycle δ and the higher is the pulse current value I_2, respectively.

After the pulse impact is over, cooling of arc column plasma occurs due to the dissipative mechanism of energy transfer, so that value T_0 decreases continuously during the entire pause duration. Characteristic time of relaxation of arc plasma temperature in the pause for the selected parameters of current modulation is equal to the value of the order of 30 μs (see Figure 2, *a*). At the pulse leading edge the plasma is heated by Joule heat source, which almost instantly reacts to a change of arc current. Here, in the case of small δ values (high values of pulse current), plasma temperature in the column center rises abruptly to values, exceeding the respective values for a DC arc, with current I_2, and then smoothly decreases during the time of the order of 20 μs (see curve 1 in Figure 2, *a*).

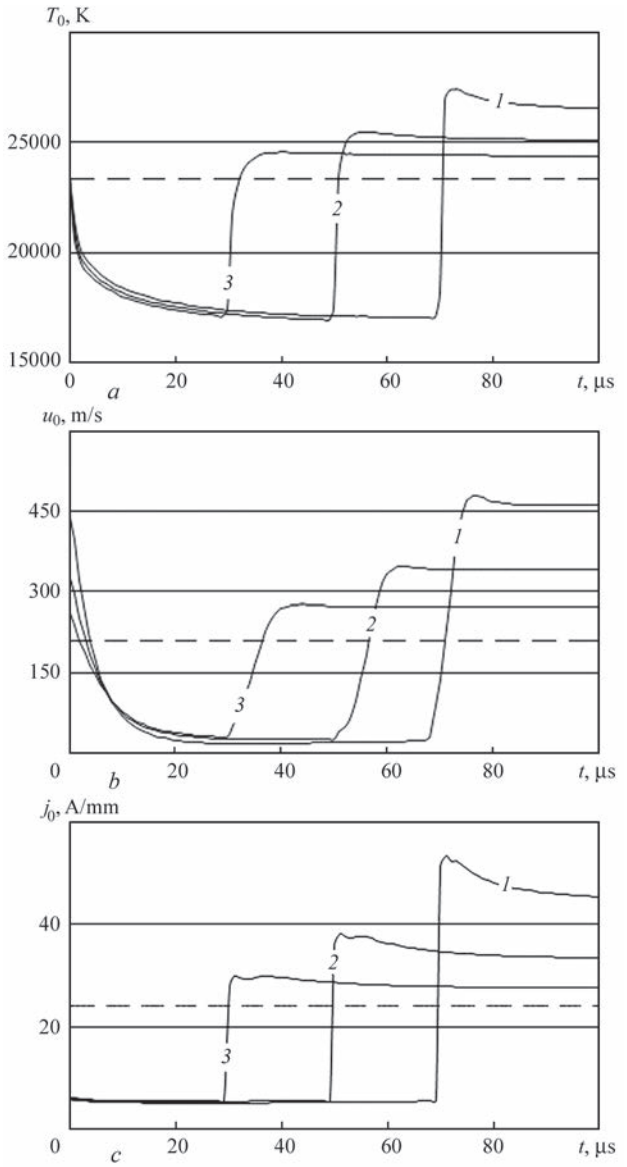

Figure 2. Time dependencies of plasma temperature (*a*), axial components of velocity (*b*) and current density (*c*) in the arc column center

A similar pattern is observed also for the velocity of plasma in the center of arc column (see Figure 2, *b*), except for value u_0 growing slower than temperature at instantaneous rise of current on the pulse leading edge. This is associated with the inertia of gas-dynamic processes in arc plasma [15]. As regards the change in time of current density in the arc column center, it decreases almost instantly at current drop on the pulse trailing edge and grows, accordingly, on the leading edge (see Figure 2, *c*). Note that at small values of δ, behaviour of values u_0 and j_0 at transition from the pause to the pulse corresponds to the above described extreme behaviour of arc plasma temperature with subsequent relaxation (see curves *1* in Figure 2, *a–c*).

We will analyze the characteristics of thermal, force and electromagnetic impact of the considered arc on the anode surface. Figure 3 shows the time dependencies of axial values of temperature T_{a0} of arc plasma column on the interface with the anode boundary layer, overpressure P_{a0} and current density j_{a0} on the anode surface, as well as the heat flux introduced by the arc into the anode q_{a0}.

Quantity T_{a0} behaves similar to plasma temperature in the arc column center, at significantly smaller values both during the pause, and during the pulse (compare Figures 2, *a* and 3, *a*). As overpressure can be presented as a sum of magnetic pressure P_m and pressure P_v due to plasma motion [15], analysis of time dependence of value P_{a0} should be performed, allowing for this circumstance. Axial value of magnetic pressure, dependent on radial distribution of current density, changes almost instantly on the pulse leading and trailing edges, reacting to the respective changes of arc current. As regards to pressure due to plasma motion, its change occurs slower, which is associated with the above-noted inertia of gas-dynamic processes in arc plasma. It leads to a two-stage change in the axial value of aggregated overpressure on the anode surface: almost instant at the first stage and slower at the second one, with characteristic relaxation time of about 10 μs during the pulse (see Figure 3, *b*).

Dynamics of the change in time of axial values of anode current density and heat flux into the anode is shown in Figure 3, *c*, *d*. Unlike the respective values

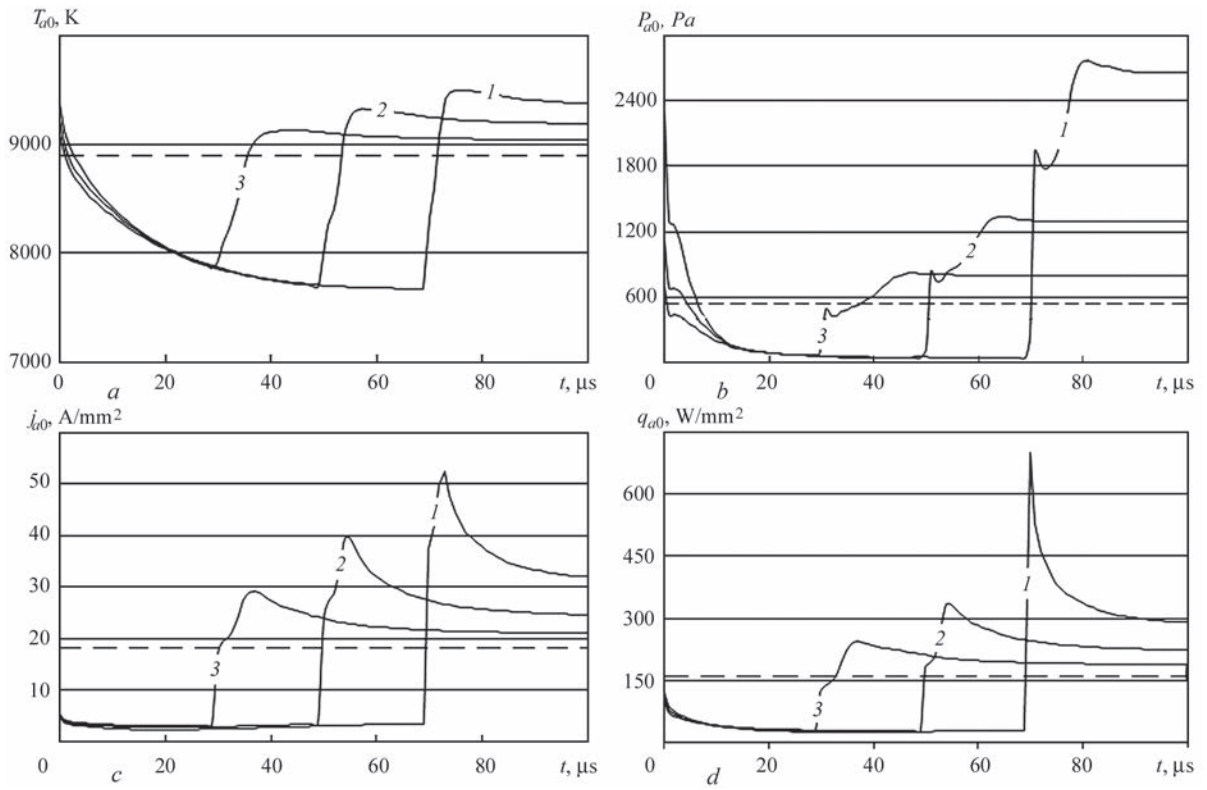

Figure 3. Time dependencies of axial values of arc plasma temperature on the interface with the anode boundary layer (*a*), overpressure (*b*) and current density (*c*) on the anode surface, as well as heat flux into the anode (*d*)

of arc plasma temperature and overpressure near the anode surface, value j_{a0} falls quickly enough on the pulse trailing edge and remains practically constant during the pause (compare Figure 3, *a*–*c*). At pulse feeding, increase of the mentioned value (similar to axial overpressure on the anode surface) occurs in two stages. At the first stage current density on the axis of the arc anode attachment rises abruptly, as at feeding of the pulse high current flows through the current channel of a small cross-section, initially remaining after the pause. At the second stage restructuring of radial distribution of plasma temperature and, hence, of its electric conductivity, takes place through convective-conductive energy transfer in arc column plasma, leading to further, slower increase of quantity j_{a0}. As a result, for all the considered duty cycles, the axial value of current density on the anode surface rises up to values, significantly exceeding the respective values for a DC arc, with current equal to I_2, and then it relaxes to them with the characteristic time of the order of 20 μs (see Figure 3, *c*). As the specific heat flux into the anode is practically proportional to anode current density [14], the change of value q_{a0} in time is similar to the change of axial value of current density on the anode surface (see Figure 3, *c*, *d*).

We will consider radial distributions of thermal, force and electromagnetic impact of a nonstationary arc on the anode surface. In study [15] it is shown

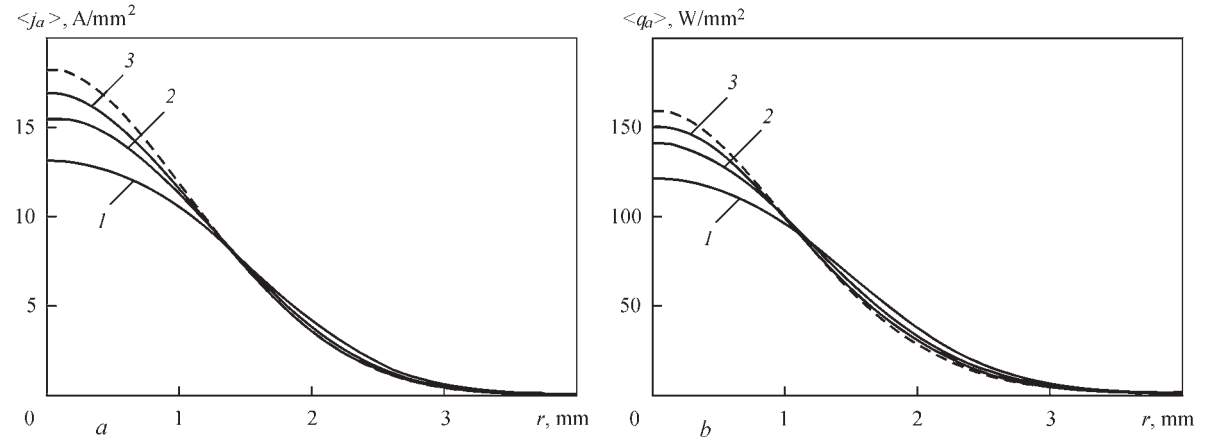

Figure 4. Radial distributions of averaged over the modulation period values of current density on the anode surface (*a*) and heat flux into the anode (*b*)

Table 2. Full heat flux into the anode

δ	$\langle Q_a \rangle$, W
0.3	1261
0.5	1212
0.7	1183
DC mode	1141

that at TIG welding with high-frequency ($f \sim 10$ kHz) pulsed modulation of current, the thermal and force impact of the arc on the surface of the metal being welded (radial distributions of heat flux into the anode and overpressure of arc plasma on its surface) can be regarded as averaged over the modulation period, as the characteristic time of the change of metal temperature and velocity in the weld pool is equal to a value of the order of 10^{-2} s, that is two orders of magnitude greater than the period of current modulation with the specified frequency.

Figure 4 gives radial distributions of anode current density $\langle j_a(r, t)\rangle$ and heat flux$\langle q_a(r, t)\rangle$, introduced into the anode, averaged over the period of arc current modulation. Respective radial distributions of magnetic pressure $\langle P_m(r, t)\rangle$ and pressure due to arc plasma motion $\langle P_v(r, t)\rangle$ on the anode surface are shown in Figure 5.

Unlike the considered above extreme change of instantaneous values of current density on the anode surface, and heat flux into the anode on the axis of the region of the arc anode attachment (see Figure 3, *c*, *d*), the dependencies given in Figure 4 demonstrate an opposite tendency, namely averaged axial values of current density and heat flux into the anode decrease at reduction of duty cycle δ. Moreover, they remain smaller than the respective values of j_{a0} and q_{a0} for a DC arc, with current equal to average value of modulated current. This is associated with the fact that at δ decrease the pause duration becomes greater, during which the anode current density and the heat flux into the anode are much lower than the respective values for an equivalent DC arc (see Figure 3, *c*, *d*).

According to the data, presented in Table 2, the averaged value of total heat flux into the anode $\left\langle Q_a \right\rangle = 2\pi \int_0^\infty \left\langle q_a(r,t) \right\rangle r dr$ unlike $\langle q_{a0}(t)\rangle$, rises at decrease of δ (at increase of pulse current) and constant average current. This feature is related to a change of filling of the profiles $\langle q_a(r, t)\rangle$, depending on the duty cycle (see Figure 4, *b*).

As regards electromagnetic impact of the arc with HFPC modulation on weld pool metal, it can also be considered as an averaged value over the modulation period [15], allowing for the fact that the expression for Lorenz force $\vec{F} = \mu^0 \vec{j} \times \vec{H}$ setting the molten metal into motion, is quadratic in current density $\vec{j}$ (magnetic field intensity $\vec{H}$). Therefore, in order to determine the spatial distribution of averaged value of electromagnetic force, it is necessary to find the distributions of the above-mentioned values at each moment of time, using the distribution of electric current density on the anode surface at the respective moment of time, then calculate the instantaneous values of $\vec{F}$ (r, z, t) and only then average over time. Here, $j_a(r, t)$ distributions should be used instead of $\langle j_a(r, t)\rangle$ distribution given in Figure 4, *a*.

Comparison of the thus calculated averaged electromagnetic force $\langle F_{mz}(r, z, t)\rangle$ in the case of the considered high-frequency (f = 10 kHz) current modulation by rectangular pulses in the form of a meander (δ = 0.5) and the respective force for an equivalent DC arc shows that the magnitude of this force in the first case turns out to be approximately 1.5 times greater than in the second case [15], and it increases at δ reduction. As this force causes molten metal motion towards the weld pool bottom, the penetrability of the arc with HFP modulation of current should become greater with decrease of the duty cycle (with I_2 increase) while maintaining I_{av}.

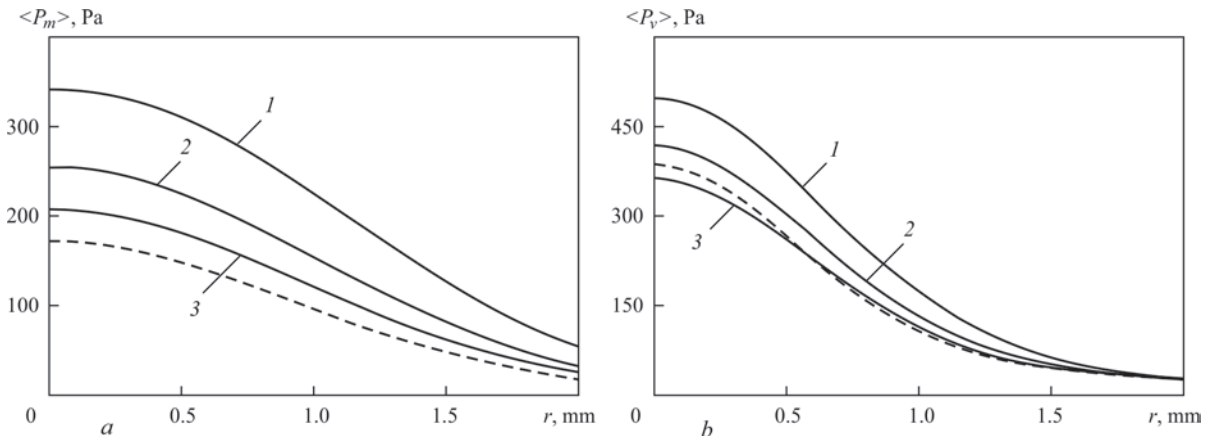

Figure 5. Radial distributions of averaged over the modulation period magnetic pressure (*a*) and pressure due to arc plasma motion (*b*) on the anode surface

As follows from the calculated data, presented in Figure 5, the averaged magnetic pressure near the surface of the anode of a nonstationary arc turns out to be significantly higher than the respective magnetic pressure for an equivalent DC arc, increasing with reduction of δ (see Figure 5, *a*). Pressure due to arc plasma motion on the anode surface, averaged over the current modulation period, also becomes higher at decrease of the duty cycle. However, its values at $\delta > 0.6$ are lower than the respective values for a DC arc at 140 A current. Average value of aggregate overpressure near the anode surface, which is a sum of $\langle P_m(r, t)\rangle$ and $\langle P_v(r, t)\rangle$ for a nonstationary arc under the considered conditions of current modulation, is higher than the overpressure of a DC arc that corresponds to the results of experimental measurement of the above quantity in [5].

Note that at determination of the shape of weld pool free surface only value P_v should be used as an essential component of arc plasma overpressure in the balance of normal stresses on the above-mentioned surface, as magnetic pressure P_m does not experience a jump when passing through arc plasma-metal interface [15]. As was already mentioned, in the case of HFPC modulation, quantity $\langle P_v(r, t)\rangle$, determining the depression of the weld pool surface, increases with δ reduction (with increase of pulse current) at constant value of average current. It promotes deeper immersion of such an arc into the metal being welded and increase of its penetrability, respectively, at I_2 increase and maintenance of the same I_{av}.

An important force factor, determining the hydrodynamic situation in the weld pool in TIG welding (alongside Lorentz and Marangoni forces) is the force of viscous friction of arc plasma flow against the anode metal surface. In the case of HFPC modulation (f = 10 kHz), the above-mentioned force, similar to P_v, can be considered as averaged over the modulation period [15]. Radial distribution of tangential stress $\langle S_v(r, t)\rangle$, generated by this force, is illustrated in Figure 6.

Calculated data given in Figure 6 shows that compared to S_v distribution for an equivalent DC arc, the maximum of averaged value of arc plasma viscous friction on the anode surface at HFPC modulation somewhat decreases in magnitude at increase of the duty cycle, and its position shifts towards smaller values of r. This is indicative of a weak effect of current modulation on the force of viscous friction of the arc plasma flow against the weld pool surface in HFPC TIG welding.

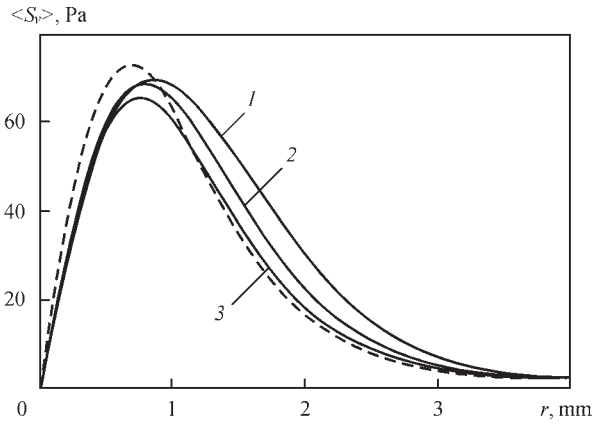

Figure 6. Radial distributions of averaged over the modulation period tangential stress, generated by the force of friction of the plasma flow on the anode surface

CONCLUSIONS

Performed numerical analysis of thermal, gas-dynamic and electromagnetic characteristics of arc plasma, as well as its impact on the anode surface, under the conditions characteristic for TIG welding with arc current modulation by rectangular pulses of different duration and amplitude (at constant value of average arc current), following at 10 kHz frequency, leads to the following conclusions:

1. At the considered modulation parameters, the current density in the arc column plasma almost instantly reacts to changes of the arc current, whereas the temperature and velocity of arc plasma have greater inertia, with the characteristic setting time of about 20 μs in the pulse and about 30 μs at transition from the pulse to the pause. Here, the values of the above-mentioned parameters are considerably higher during the pulse, that during the pause, and they are the greater, the smaller the duty cycle (the higher the pulse current).

2. Axial values of current density on the anode surface and heat flux to the anode, averaged over the period of arc current modulation, decrease at reduction of the duty cycle for the considered modulation conditions. Moreover, they remain smaller than the respective values for a DC arc at current equal to average value of modulated current. Here, the full heat flux into the anode, contrarily, is greater than the respective value for an equivalent DC arc, increasing with reduction of the duty cycle (with increase of pulse current).

3. Pressure on the anode surface due to arc plasma motion, averaged over the current modulation period, increases with reduction of the duty cycle and at $\delta < 0.6$ it becomes greater than the respective pressure for a DC arc at current equal to average value of modulated current. As a result, shortening of the pulse duration and the respective increase of current modulation amplitude in welding by an arc with a refractory cathode leads to increase of the depression of weld pool surface that promotes deeper immersion of the arc into the metal being welded and increase of its penetrability. As regards the force of viscous friction of arc plasma flow driving the surface layers of weld pool metal from its center to the

periphery, thus increasing the width of the penetration zone by reducing its depth, it practically does not differ from the respective force applied to the melt surface by plasma of an equivalent DC arc.

4. Evaluation of an averaged force impact of the considered nonstationary arc on the welded metal melt is indicative of a considerable increase (compared to an equivalent DC arc) of the volume electromagnetic force, driving the melt and causing the convective heat transfer from the surface towards the weld pool bottom, that also promotes greater penetration depth in HFPC TIG welding.

ACKNOWLEDGMENTS

This work was carried out with the financial support of the German Research Foundation DFG Project No. 390246097/RE2755/51-1 "Investigation of the influence of non-stationary processes in the arc plasma on the penetration depth during high frequency TIG welding". The authors wish to express their thanks for this funding.

REFERENCES

1. (2011) Welding fundamentals and processes. Ed. by T.J. Lienert, S.S. Babu et al. ASM Handbook, Ohio, USA. ASM Int.
2. Leither, R.E., McElhinney, G.H., Pruitt E.L. (1973) An investigation of pulsed GTA welding variables. *Welding J., Res. Suppl*., **9**, 405s–410s.
3. Omar, A.A., Lundin, C.D. (1979) Pulsed plasma-pulsed GTA arcs: A study of the process variables. *Welding J., Res. Suppl*., **4**, 97s–105s.
4. Saedi, H.R., Unkel, W. (1988) Arc and weld pool behavior for pulsed current GTAW. *Welding J., Res. Suppl*., **11**, 247s–255s.
5. Onuki, J., Anazawa, Y., Nihei, M., et al. (2002) Development of a new high-frequency, high-peak current power source for high constricted arc formation. *Japan J. Appl., Phys*., **41**, 5821–5826.
6. Karunakaran, N., Balasubramanian, V. (2011) Effect of pulsed current on temperature distribution, weld bead profiles and characteristics of gas tungsten arc welded aluminum alloy joints. *Transact. Nonferrous Met. Soc. China*, **21**, 278–286.
7. Cunha, T.V.d., Louise-Voigt, A., Bohorquez, C.E.N. (2016) Analysis of mean and RMS current welding in the pulsed TIG process. *J. of Materials Proc. Technology*, **231**, 449–455.
8. Silva, D.C.C., Scotti, A. (2017) Using either mean and RMS values to represent current in modeling of arc welding bead geometries. *J. of Materials Proc. Technology*, **240**, 382–387.
9. Kim, W.H., Na, S.J. (1998) Heat and fluid flow in pulsed current GTA weld pool. *Int. J. of Heat and Mass Transfer*, Vol. 41(Issue 21), 3213–3227.
10. Wu, C.S., Zheng, W., Wu, L. (1999) Modeling the transient behaviour of pulsed current tungsten-inert-gas weld pools. Modelling and Simul. *Mater. Sci. Eng*., 7(**1**), 15–23.
11. Traidia, A., Roger, F., Guyot, E. (2010) Optimal parameters for pulsed gas tungsten arc welding in partially and fully penetrated weld pools. *Int. J. of Thermal Sci*., **49**, 1197–1208.
12. Krivtsun, I., Demchenko, V., Krikent, I. et al. (2015) Distributed and integrated characteristics of the near-anode plasma of the welding arc in TIG and Hybrid (TIG + CO_2 Laser) welding. In: *Mathematical Modelling of Weld Phenomena 11*. Techn. Universitat Graz, Graz, Austria, 837–874.
13. Krivtsun, I., Demchenko, V., Lesnoi, A. et al. (2010) Modelling of electromagnetic processes in system "welding arc–evaporating anode". Pt 1: Model of anode region. *Sci. and Technol. of Welding & Joining*, 15(**6**), 457–463.
14. Semenov, I.L., Krivtsun, I.V., Reisgen, U. (2016) Numerical study of the anode boundary layer in atmospheric pressure arc discharges. *J. Phys. D: Appl. Phys*., 49(**10**), 105204.
15. Demchenko, V.F., Boi, U., Krivtsun, I.V., Shuba, I.V. (2017) Effective values of electrodynamic characteristics of the process of nonconsumable electrode welding with pulse modulation of arc current. *The Paton Welding J*., **8**, 2–11. DOI: https://doi.org/10.15407/tpwj2017.08.01
16. Sydorets, V.N., Krivtsun, I.V., Demchenko, V.F. et al. (2016) Calculation and experimental research of static and dynamic volt-ampere characteristics of argon arc with refractory cathode. *The Paton Welding J*., **2**, 2–8.
17. Wendelstorf, J., Simon, G., Decker, I. et al. (1997) Investigation of cathode spot behavior of atmospheric argon arcs by mathematical modeling. In: *Proc. of the 12th Int. Conf. on Gas Discharges and their Applications (Germany, Greifswald, 1997)*, Vol. 1, 62–65.
18. Benilov, M.S., Marotta, A. (1995) A model of the cathode region of atmospheric pressure arcs. *J. Phys. D: Appl. Phys*., Vol. 28, 1869–1882.
19. Cressault, Y., Murphy, A.B., Teulet, Ph. et al. (2013) Thermal plasma properties for Ar–Cu, Ar–Fe and Ar–Al mixtures used in welding plasma processes: II . Transport coefficients at atmospheric pressure. *J. Phys. D: Appl. Phys*., Vol. 46, 415207.
20. Essoltani, A., Proulx, P., Boulos, M.I. et al. (1994) Volumetric emission of argon plasma in the presence of vapours of Fe, Si and Al. *Plasma Chem. and Plasma Proc*., 14(**4**), 437–450.

ORCID

I. Krivtsun: 0000-0001-9818-3383
I. Krikent: 0000-0002-4196-6800
U. Reisgen: 0000-0003-4920-2351
O. Mokrov: 0000-0002-9380-6905
R. Sharma: 0000-0002-6976-4530

CONFLICT OF INTEREST

The Authors declare no conflict of interest

CORRESPONDING AUTHOR

I. Krivtsun
E.O. Paton Electric Welding Institute of the NASU
11 Kazymyr Malevych Str., 03150, Kyiv, Ukraine
E-mail: krivtsun@paton.kiev.ua

SUGGESTED CITATION

I. Krivtsun, V. Demchenko, I. Krikent, U. Reisgen, O. Mokrov, R. Sharma (2022) Characteristics of HFPC arc with refractory cathode. *The Paton Welding J*., **3**, 9–18.

JOURNAL HOME PAGE

https://pwj.com.ua/en

Received: 13.04.2022
Accepted: 16.05.2022